doi:10.1093/scan/nst029 SCAN (2014) 9, 671–680

# Neural correlates of impaired emotion processing in manifest Huntington's disease

Imis Dogan,[1,2,3] Christian Saß,[1,4] Shahram Mirzazade,[1,2,3] Alexandra Kleiman,[1,2,3] Cornelius J. Werner,[1,2] Anna Pohl,[1,3,5] Johannes Schiefer,[1] Ferdinand Binkofski,[2,3,6] Jörg B. Schulz,[1,3] N. Jon Shah,[1,2,3] and Kathrin Reetz[1,2,3]

[1]Department of Neurology, RWTH Aachen University, Pauwelsstraße 30, D-52074 Aachen, Germany, [2]Institute of Neuroscience and Medicine, Research Center Jülich GmbH, Wilhelm-Johnen-Straße, D-52428 Jülich, Germany, [3]JARA – Translational Brain Medicine, Aachen/Jülich, Germany, [4]Department of Neurology—Huntington Center, University Hospital Münster, University of Münster, Albert-Schweitzer-Straße 33, D-48149 Münster, Germany, [5]Department of Psychiatry, Psychotherapy, and Psychosomatics, RWTH Aachen University, Pauwelsstraße 30, D-52074, and [6]Section for Cognitive Neurology, Department of Neurology, RWTH Aachen University, Pauwelsstraße 30, D-52074 Aachen, Germany

**The complex phenotype of Huntington's disease (HD) encompasses motor, psychiatric and cognitive dysfunctions, including early impairments in emotion recognition. In this first functional magnetic resonance imaging study, we investigated emotion-processing deficits in 14 manifest HD patients and matched controls. An emotion recognition task comprised short video clips displaying one of six basic facial expressions (sadness, happiness, disgust, fear, anger and neutral). Structural changes between patients and controls were assessed by means of voxel-based morphometry. Along with deficient recognition of negative emotions, patients exhibited predominantly lower neural response to stimuli of negative valences in the amygdala, hippocampus, striatum, insula, cingulate and prefrontal cortices, as well as in sensorimotor, temporal and visual areas. Most of the observed reduced activity patterns could not be explained merely by regional volume loss. Reduced activity in the thalamus during fear correlated with lower thalamic volumes. During the processing of sadness, patients exhibited enhanced amygdala and hippocampal activity along with reduced recruitment of the medial prefrontal cortex. Higher amygdala activity was related to more pronounced amygdala atrophy and disease burden. Overall, the observed emotion-related dysfunctions in the context of structural neurodegeneration suggest both disruptions of striatal-thalamo-cortical loops and potential compensation mechanism with greater disease severity in manifest HD.**

**Keywords:** Huntington's disease; emotion processing; functional MRI; voxel-based morphometry; neurodegenerative disorders

## INTRODUCTION

Huntington's disease (HD) is an autosomal-dominantly inherited neurodegenerative disorder caused by an expanded CAG repeat on chromosome 4p. The earliest neuropathological changes are found in the striatum starting several years before symptom manifestation (Aylward *et al.*, 2004; Paulsen *et al.*, 2010), and eventually leading to widespread brain atrophy (Vonsattel, 2008). Symptom manifestation is conventionally defined by the onset of motor symptoms, though the clinical phenotype of HD is complex and further encompasses psychiatric and cognitive dysfunctions, including early impairment in emotion processing (Henley *et al.*, 2011; Paulsen, 2011).

The ability to accurately recognize and infer the emotional states of others is crucial for adequate social behavior and interpersonal interactions. There has been an increasing interest on emotion processing in HD to improve our understanding of pervasive cognitive and psychiatric disturbances and as a potential biomarker to monitor disease-progression and disease-modifying treatments (Tabrizi *et al.*, 2009). Behavioral findings in pre-manifest HD have been inconsistent, though deficits in disgust recognition were reported more commonly (Gray *et al.*, 1997; Hennenlotter *et al.*, 2004; Sprengelmeyer *et al.*, 2006). Manifest patients seem to feature a more generalized impairment in emotion recognition with negative facial expressions (particularly anger, fear and disgust) being more severely affected than happiness or surprise (for review see Henley *et al.*, 2011). The neural substrates underlying these deficits were mostly investigated by correlative structural magnetic resonance imaging (MRI) studies (Johnson *et al.*, 2007; Kipps *et al.*, 2007; Henley *et al.*, 2008; Ille *et al.*, 2011; Scahill *et al.*, 2011). Importantly, disease-related behavioral manifestations are less likely to be sufficiently explained by distinct regional tissue degeneration, but rather depend on the complex interactions within multiple brain circuits or disruptions of the same (Paulsen, 2009). To date, two functional MRI (fMRI) studies have investigated the neural correlates of emotion processing in pre-manifest mutation carriers: using an implicit emotion perception task with disgusted and surprised facial expressions, Hennenlotter *et al.* (2004) reported decreased brain activity in the left anterior mid-insula during disgust processing in nine pre-manifest HD subjects compared with controls, explaining the deficient disgust recognition in the HD group. In a recently published fMRI study, Novak *et al.* (2012) used a similar task in 16 pre-manifest subjects and revealed, in the absence of behavioral deficits, altered neural activity in widely distributed networks including prefrontal, parietal, insular and cingulate cortices during disgust, anger and happiness processing. However, significant group differences were only observed after controlling for gene dosage (CAG repeats or probability of disease onset within 5 years), which the authors explained with the heterogeneous nature of HD (Novak *et al.*, 2012). Since behaviorally emotion recognition deficits seem to converge to a more general impairment in the manifest stage, emotion-related functional alterations in conjunction with progressive structural degeneration may also become more pervasive after symptom manifestation. Understanding emotional disturbances is of particular interest in early manifest HD given its clinical relevance, impact on quality of life and potential therapeutic options. Thus, complementing findings in pre-manifest HD, we aimed at investigating the neural correlates of emotion-processing deficits in the symptomatic

Received 20 September 2012; Accepted 21 February 2013
Advance Access publication 11 March 2013

We sincerely thank all our patients and control subjects for their enduring collaboration and interest in this research. We also thank Daniela Probst for her excellent recruitment help and Harshal Patel for his assistance in Matlab programming. This work was supported by the Excellence Initiative of the German Research Foundation [DFG ZUK32/1 to K.R.] and the Interdisciplinary Center for Clinical Research within the faculty of Medicine at the RWTH Aachen University [IZKF N4-4 to K.R.].

Correspondence should be addressed to Kathrin Reetz, Department of Neurology, RWTH Aachen University, Pauwelsstrasse 30, D-52074 Aachen, Germany. Tel.: +49-241-80-36516; Fax: +49-241-80-33-36516. E-mail: kreetz@ukaachen.de

stage of HD. In the current fMRI study, we examined the processing of five basic emotions (i.e. fear, anger, disgust, sadness and happiness) in an event-related emotion recognition paradigm displaying video sequences of vivid facial expressions. We expected to find deficient accuracy in the recognition of negative emotions and abnormal patterns of neural activity in response to emotional stimuli in patients, particularly in limbic networks. Additionally, we investigated the impact of structural alterations on emotion-related activity patterns in HD.

## METHODS

### Participants

Fourteen manifest HD patients were recruited from our Huntington Outpatient Clinic (Department of Neurology, RWTH Aachen University). The control group comprised 14 healthy volunteers with no history of neurological or psychiatric diseases matched for age, gender and handedness in a pair-wise manner and did not significantly differ from the HD group in educational level (Table 1). All subjects gave their written informed consent for participation in this study, which was approved by the local ethics committee according to the declaration of Helsinki.

Participants were examined using the Unified Huntington's Disease Rating Scale (UHDRS; Huntington Study Group 1996) for each subscale (motor, function, behavior and cognition), the Mini-Mental State Exam (MMSE; Folstein *et al.*, 1975), and a modified version of the Wisconsin Card Sorting Test (mWCST; Nelson, 1976; Truong, 1993). Most patients were in an early disease stage (stage I: 6 and stage II: 6), two patients in a moderate stage III (Shoulson and Fahn, 1979). Four patients showed depressive mood symptoms in the UHDRS-behavior assessment, but none of them was suffering a severe depressive episode at the time of study participation. All participants were autonomous (UHDRS-independence scale $\geq$75%) and showed no signs of dementia. UHDRS-cognitive assessment revealed mild to moderate impairments in patients, but no significant differences compared with controls were found regarding executive functioning as measured by perseverative errors in the mWCST. To measure the current self-reported experience with different emotional valences, participants completed the Disgust Scale (Haidt *et al.*, 1994) and Emotional-Experience-and-Regulation questionnaire (Benecke *et al.*, 2008), which revealed no significant group differences in the experience of basic emotions used in the fMRI task. Additionally, subjects completed the Positive and Negative Affect Scales (PANAS; Watson *et al.*, 1988) and Snaith Irritability Depression Anxiety Scale (IDA; Snaith *et al.*, 1978). Here, patients scored significantly higher than controls in the PANAS-negative affect, IDA-depression, anxiety and inward irritability scales (Table 1). To assess the burden of disease pathology and its influence on neural activity, we used the index of disease-burden based on the formula age $\times$ [CAG $-$ 35.5] (Penney *et al.*, 1997). This score provides a measure of genetic disease load while taking in account subjects' current age and was shown to strongly correlate with HD-related clinical features (Tabrizi *et al.*, 2009).

**Table 1.** Demographics, clinical and neuropsychological scores for HD patients and controls

| | HD patients ($n = 14$) | | Controls ($n = 14$) | | *P*-value |
|---|---|---|---|---|---|
| | Mean | SD | Mean | SD | |
| Age (in years) | 43.9 | 8.9 | 44.3 | 8.9 | 0.900 |
| Gender (male/female) | 8/6 | | 8/6 | | |
| Handedness (R/L)[a] | 12/2 | | 12/2 | | |
| Education (ISCED) | 3.1 | 0.9 | 3.9 | 1.0 | 0.062[b] |
| CAG repeat length | 45.1 | 2.3 | n.a. | n.a. | |
| Disease burden[c] | 408.9 | 72.0 | n.a. | n.a. | |
| MMSE | 27.5 | 2.1 | 29.3 | 0.6 | 0.007 |
| UHDRS | | | | | |
| Motor | 33.8 | 17.9 | 0.6 | 0.8 | <0.001 |
| TFC | 9.6 | 2.7 | 13.0 | 0.0 | <0.001[b] |
| Behavior | 15.5 | 13.6 | 2.4 | 3.2 | 0.003 |
| Cognitive | 200.9 | 69.5 | 335.0 | 44.1 | <0.001 |
| mWCST | | | | | |
| Errors | 14.8 | 7.0 | 9.3 | 7.0 | 0.046 |
| Perseverative errors | 6.8 | 5.0 | 4.1 | 5.7 | 0.206 |
| IDA[d] | | | | | |
| Depression | 4.0 | 2.9 | 1.7 | 1.4 | 0.024 |
| Anxiety | 4.1 | 2.2 | 1.0 | 1.1 | <0.001 |
| Outward irritability | 3.3 | 2.3 | 1.6 | 2.0 | 0.061 |
| Inward irritability | 2.3 | 1.5 | 1.2 | 1.2 | 0.046 |
| PANAS[e] | | | | | |
| Positive affect | 31.1 | 9.3 | 37.7 | 6.5 | 0.078 |
| Negative affect | 23.2 | 6.2 | 14.7 | 4.6 | 0.002 |
| EER[d] | | | | | n.s. |
| Emotion experience | | | | | |
| Interest | 3.1 | 1.6 | 4.5 | 0.6 | 0.017[b] |
| Emotion regulation | | | | | n.s. |
| Reflection | 2.3 | 1.6 | 4.1 | 0.8 | 0.002[b] |
| Empathy | 2.2 | 1.2 | 3.8 | 1.5 | 0.010[b] |
| Disgust scale | 81.9 | 29.5 | 69.0 | 18.1 | 0.179 |

[a]Based on the Edinburgh Inventory (Oldfield, 1971). [b]Mann–Whitney U-tests (remaining group comparisons assessed with two-sample *T*-tests). [c]Age x (CAG–35.5) based on Penney *et al.* (1997). [d]$n = 12$. [e]$n = 10$. SD, standard deviation; ISCED, International Standard Classification of Education (1997); MMSE, Mini-Mental State Examination; UHDRS, Unified Huntington's Disease Rating Scale; TFC, Total Functional Capacity Score; mWCST, Modified Wisconsin Card Sorting Test; PANAS, Positive and Negative Affect Scale; IDA, Irritability Depression Anxiety Scale; EER, emotion experience and regulation questionnaire (only significant group comparisons with uncorrected $P < 0.05$ are reported); n.a., not applicable; n.s., not significant.

### Emotion recognition paradigm

For the fMRI paradigm, stimulus material consisted of short video clips displaying different facial expressions performed by 24 actors and was used in previous fMRI studies (Anders *et al.*, 2012; Kircher *et al.*, 2012). Actors were filmed in portrait format including their head and shoulders in front of a gray background. The actors' hair was fixed and covered with a black scarf. Video clips were cut to a length of 3 s with each sequence starting immediately with the onset of the facial gesture and terminating at the height of the emotional expression. Actors produced several instances of affective and neutral expressions, which were rated according to the shown expression and intensity of the expressed emotion by 30 naive observers in a prior behavioural study. For the present fMRI study, we selected video clips of 20 actors (10 female) displaying fear, sadness, disgust, anger, happiness and neutral expressions as a control condition. The most accurate expression of each category per actor (i.e. videos with the highest recognition rate) but with medium intensity was selected. We opted for these criteria in order to minimize task difficulty for patients while avoiding ceiling effects with full-blown facial expressions in controls. Hence, the emotion recognition task comprised 20 videos of each of the five emotional and neutral expressions. In an event-related design, each video was presented against a black screen for 3 s followed by the instruction to categorize the video by pressing one of six buttons according to the possible facial expressions, which were displayed on the screen labeled in the same order as the respective response buttons. Subjects were asked to respond within 3 s before the next video was presented in a pseudo-randomized order (four randomization sequences were randomly assigned to the participants) with an inter-stimulus interval of 1 s (fixation cross), giving the fMRI paradigm a total duration of $\sim$15 min. Prior to scanning, each subject was given enough time to familiarize with the task with a different video sample derived from the remaining set of four actors ($\sim$10–15 min).

### MRI data acquisition

MR images were acquired with a 3-Tesla Trio MR scanner (Siemens Medical Systems, Erlangen, Germany). T2*-weighted images were obtained using echo-planar imaging (EPI) parallel to the AC/PC-line (TR = 2200 ms, TE = 30 ms, FoV = 200 mm, 64 × 64 matrix, 36 slices and slice thickness = 3.1 mm). High-resolution T1-weighted images were acquired using a magnetization-prepared rapid gradient-echo sequence (TR = 1900 ms, TE = 2.52 ms, TI = 900 ms, FoV = 250 mm, 256 × 256 matrix, 176 sagittal slices and slice thickness = 1 mm).

### Analysis of functional MRI data

Image processing and statistical analyses were performed using Statistical Parametric Mapping software (SPM8, www.fil.ion.ucl.ac.uk/spm) implemented in MATLAB7.6 (Mathworks Inc., Natick, MA, USA). Functional images were realigned to the mean EPI volume, which was coregistered with the T1-weighted anatomical image of each subject. After spatial normalization to the SPM8 EPI standard template, images were smoothed with an 8 mm full width at half maximum (FWHM) isotropic Gaussian kernel. Single subject (first level) and group analyses (second level) were performed within the framework of the general linear model (Friston *et al.*, 1995). On the first level, the hemodynamic response function was convolved with the onset of every event, and realignment parameters were entered as regressors of no interest to account for motion artifacts. Contrast images were generated for each of the five emotion conditions *vs* control condition (emotion > neutral) for each subject, which were entered in a repeated-measures ANCOVA on the second level (within-subject factor: emotional expression; between-subjects factor: HD *vs* controls) by including age as a covariate. Activation differences between patients and controls were assessed using *t*-contrasts. Emotion-related regions of interest (ROI), based on literature on emotion recognition in HD and meta-analyses of functional imaging studies in healthy subjects (Phan *et al.*, 2002; Fusar-Poli *et al.*, 2009), included the caudate, putamen, amygdala, hippocampus and parahippocampal gyrus, insula, anterior cingulate (ACC), orbito-frontal (OFC) and medial prefrontal cortex (mPFC). We further included the thalamus as a ROI, as both thalamic atrophy in co-variation with cognitive performance and dysfunctional thalamic metabolism seem to be an early feature in HD (Kassubek *et al.*, 2005; Feigin *et al.*, 2007). ROI defined by cytoarchitectonic probabilistic maps were available for the amygdala, hippocampus (Amunts *et al.*, 2005) and thalamus (Behrens *et al.*, 2003), which were derived separately for each hemisphere from the Anatomy-Toolbox (Eickhoff *et al.*, 2005, 2006). Masks for remaining ROI were created using the WFU-PickAtlas (Tzourio-Mazoyer *et al.*, 2002; Maldjian *et al.*, 2003). For ROI analyses, significance was accepted for clusters of more than five contiguous voxels exceeding a statistical threshold of $P < 0.05$ family-wise error (FWE) corrected. Outside our ROI, results are reported after FWE cluster-level correction with $P < 0.05$ (uncorrected at the voxel-level with $P < 0.001$) across the whole brain.

### Analysis of structural MRI data: voxel-based morphometry

Regional gray matter (GM) changes in HD patients relative to controls were analyzed by means of voxel-based morphometry (VBM; Ashburner and Friston, 2000; Good *et al.*, 2001) using the VBM8 toolbox (http://dbm.neuro.uni-jena.de/vbm). Briefly, T1-weighted images were spatially normalized by high-dimensional warping (DARTEL) with a standard template and segmented into GM, white matter and cerebrospinal fluid. To correct for individual brain sizes and allow comparing the absolute amount of tissue volume (Good *et al.*, 2001), voxel values were multiplied (modulated) by the non-linear component of the Jacobian determinant derived from the spatial normalization. Finally, modulated GM images were smoothed with a Gaussian kernel of 8 mm FWHM. GM differences between patients and controls were tested using two-sample *T*-tests and by including age as a nuisance covariate. Results were thresholded at $P < 0.05$ (FWE-corrected) within ROI and across the whole brain. In case of an overlap between functional and structural alterations and to investigate functional activity outside of atrophic regions, we created two binary masks: one mask blanked all significant voxels in the VBM-ROI analyses and in the second mask, significant VBM results across the whole brain were excluded. Functional activation differences between patients and controls were reanalyzed as reported above but after explicitly masking statistical parametric maps with each of these created masks. That is, differences in BOLD response between patients and controls were restricted to those voxels not affected by significant GM changes (Wolf *et al.*, 2009).

### Correlation analyses

We conducted exploratory *post hoc* correlation analysis to assess systematic covariations between neural activity, GM volumes and behavioral variables. For this, we extracted GM values and functional parameter estimates for each significant ROI per subject, and correlated functional activity with GM volumes in respective ROI, emotion recognition accuracies in the fMRI paradigm and clinical variables (i.e. CAG repeats, disease-burden, UHDRS-subscores, PANAS-negative affect, IDA depression and anxiety scores). Extracted data were adjusted for age since age was included as a nuisance variable in all statistical analyses. As most of imaging and behavioral data did not indicate significant violations of normal distribution (Kolmogorov–Smirnov tests $P > 0.05$), we computed Pearson's product–moment coefficients where appropriate thresholded at $P < 0.05$ (uncorrected).

## RESULTS

### Behavioral performance in emotion recognition task

Average emotion recognition accuracy was above-chance level in both groups (HD: 33–83%, controls: 78–88%; chance 16%). Patients performed significantly worse than controls in the recognition of all negative emotions (disgust, fear, sadness and anger) but showed no significant differences in recognizing neutral expressions (Table 2). We further found a tendency of impaired recognition of happiness in patients, which did not survive Bonferroni correction for multiple comparisons (uncorrected $P = 0.042$). Note that ceiling effects were observed for happiness recognition in controls. Within group analyses of recognition accuracies for negative emotions showed no significant differences in the HD group (repeated-measures ANOVA: $F_{3,39} = 2.65$, $P = 0.850$), indicating that there was no disproportionate impairment in a particular negative emotion. Additionally, analyses of error types within the HD group revealed significant effects for disgust ($F_{2.9,37.1} = 10.92$, $P < 0.001$) and sadness ($F_{2.3,29.7} = 4.58$, $P = 0.015$). In particular, disgust was more frequently misinterpreted as anger, fear or sadness than as happiness or neutral by patients (*post hoc* paired *T*-tests: $T_{13} \geq 1.46$, $P \leq 0.001$; respectively, and corrected for multiple comparisons); compared with controls, patients misinterpreted disgust videos as fear or anger more frequently than controls (two-sample *T*-tests: $T_{16.4} = 3.07$, $P = 0.007$ and $T_{15.6} = 4.56$, $P \leq 0.001$). Error analysis for the recognition of sadness showed that patients misclassified sad videos more frequently as fear, anger and neutral expressions than as happiness ($T_{13} \geq 4.55$, $P \leq 0.001$); though compared with controls false positives for sadness were only significant for neutral appraisals ($T_{13.8} = 4.98$, $P \leq 0.001$), indicating that patients more frequently judged sad videos as neutral expressions than controls.

**Table 2.** Percentage of correctly recognized facial expressions in the emotion recognition task

| | HD patients ($n = 14$) | | Controls ($n = 14$) | | Uncorrected $P$-value[a] |
|---|---|---|---|---|---|
| | Mean % | SD | Mean % | SD | |
| Fear | 41.4 | 22.4 | 92.9 | 5.8 | <0.001 |
| Anger | 37.5 | 18.2 | 65.4 | 10.5 | <0.001 |
| Disgust | 40.4 | 26.1 | 80.7 | 8.1 | <0.001 |
| Sadness | 37.1 | 18.6 | 71.1 | 16.9 | <0.001 |
| Happiness | 87.1 | 21.3 | 100.0 | 0.0 | 0.042 |
| Neutral | 93.6 | 8.2 | 96.8 | 4.2 | 0.203 |
| Total | 56.2 | 14.2 | 84.5 | 3.1 | <0.001 |

[a]Two-sample *T*-tests.

### Voxel-based morphometry

Whole-brain analysis of volume reductions in HD patients compared with controls revealed GM atrophy in patients in the bilateral putamen and caudate extending to the thalamus and pallidum, bilateral hippocampus, left premotor (PMC) and primary motor cortex (M1), middle temporal gyrus, right inferior parietal cortex and in visual cortices (Table 3 and supplementary Figure S1; cf. Figure 2). There were no significant volume increases in patients compared with controls. ROI analysis showed significant GM atrophy in most of the pre-defined areas: in the bilateral caudate, putamen, amygdala, thalamus, hippocampus, insula, left parahippocampal gyrus and left OFC (Supplementary Table S1; cf. Figure 1).

### Functional imaging results

During video clips displaying *fear*, we found decreased BOLD response in patients relative to controls in the left centromedial amygdala, right hippocampus, bilateral medial thalamic nuclei connecting to prefrontal and temporal cortices (Behrens *et al.*, 2003), ventral and dorso-ventral putamen, right ventral caudate, left dorsal mid-insula and right ACC (Table 4 and Figure 1A). For *anger* the right hippocampus, bilateral medial thalamus, ventral putamen and left mPFC were less activated in patients compared with controls (Table 4 and Figure 1B). During videos expressing *disgust*, we observed less recruitment in patients in the bilateral ventral putamen, dorso-ventral caudate, posterior insula and inferior OFC (Table 4 and Figure 1C). The left mPFC was also less recruited during *sadness* (Table 4 and Figure 1E). For *sadness*, we additionally observed increased BOLD response in patients compared with controls in the bilateral laterobasal amygdala, hippocampus and right parahippocampal gyrus (Table 4 and Figure 1D).

Outside of predicted ROI, we found less neural activity for *fear*, *anger* and *disgust* in patients compared with controls in the inferior frontal gyrus, left PMC, M1 and somatosensory cortex (SI) (Table 5 and Figure 2). During *fear* videos, patients also showed decreased BOLD response in the left supplementary motor area, left middle and bilateral posterior cingulate cortex, bilateral precuneus, superior parietal cortex, superior and middle temporal gyri. The left central opercular cortex, bilateral cuneus, visual areas, cerebellum and right pallidum were less recruited in patients during *fear* and *anger* videos, and inferior and middle temporal gyri during *anger* and *disgust*. For *happiness*, we only found significant group differences in extrastriate visual cortices. During *sadness*, there were no other group differences in neural activity outside of predicted ROI (note that higher activity in patients in the left amygdala and hippocampus was also significant across the whole brain, Figure 2). We additionally performed an analysis comparing 11 HD patients with an average emotion recognition accuracy above 50% and 11 matched controls. Here, most of the reduced activity patterns in the patient group remained robust; additionally we observed increased activity for sadness in the ACC and middle frontal gyrus.

**Table 3.** Significant GM volume reductions in HD patients compared with controls

| Anatomical region | | MNI coordinates | | | *Z* |
|---|---|---|---|---|---|
| | | *x* | *y* | *z* | |
| Putamen | L | −21 | 17 | 1 | 7.49 |
| | R | 18 | 10 | 1 | 7.06 |
| Caudate, extends to thalamus | L | −10 | 16 | 4 | 7.41 |
| | R | 14 | −3 | 19 | 6.80 |
| Hippocampus | L | −30 | −13 | −11 | 5.03 |
| | R | 20 | 3 | −24 | 5.02 |
| Premotor cortex [BA 6] | L | −39 | −15 | 55 | 5.19 |
| Primary motor cortex [BA 4a] | L | −36 | −19 | 55 | 5.26 |
| Inferior parietal cortex | R | 64 | −27 | 27 | 5.21 |
| Middle temporal gyrus | L | −48 | −60 | 21 | 5.56 |
| Lingual gyrus [BA 17] | L | −4 | −82 | 0 | 5.27 |
| Middle occipital gyrus [BA 18] | L | −26 | −96 | 10 | 5.12 |
| | R | 20 | −84 | −11 | 5.13 |

VBM results are FWE corrected at $P < 0.05$ across the whole brain; *Z*, maximum *Z*-value for the anatomical area; BA, Brodmann area.

### Functional imaging results outside of atrophic regions

To account for brain atrophy, we reanalyzed functional imaging data after excluding all voxels showing significant GM differences between patients and controls in the VBM analyses. Functional group differences were similar as reported above in the ROI analyses and across the whole brain, with the following exceptions: group differences in the left amygdala for *fear*, right putamen for *anger* and right caudate for *fear* and *disgust* could not be replicated. The signal increase in the amygdala in patients compared with controls during *sadness* diminished substantially, but was still significant in the left hemisphere. Across the whole brain, group differences in the occipital cortex for *anger* and *happiness*, and in the pallidum for *fear* did not survive cluster-level FWE correction (supplementary Table S2).

### Correlation analyses

Thalamic volumes in HD patients correlated positively with thalamic activity during *fear* in each hemisphere (left: $r = 0.632$, $P = 0.015$; right: $r = -0.557$, $P = 0.038$; Figure 3A), indicating that lower functional activity in the thalamus was associated with more pronounced thalamic atrophy. Similarly, GM loss in the left mPFC co-varied with lower functional activity in this region during *sadness* ($r = 0.542$, $P = 0.045$). In the left amygdala, we found a negative correlation between GM volumes and BOLD response during *sadness* ($r = -0.565$, $P = 0.035$), i.e. higher functional activity in the amygdala was related to amygdala atrophy in patients.

Amygdala activity during *sadness* further correlated negatively with recognition accuracies of *sadness* in patients ($r = -0.566$, $P = 0.035$), while we found a positive association between amygdala activity and recognition of *fear* in controls ($r = 0.741$, $P = 0.002$). Higher amygdala activity during *fear* and *sadness*, and hippocampal activity during *fear* were associated with higher disease-burden scores ($r = 0.651$ to $0.668$, $P \leq 0.012$). Higher CAG repeats were associated with stronger insular recruitment during *disgust* ($r = 0.617$, $P = 0.019$; Figure 3B), indicating an increase in functional activity with higher genetic load in HD.

## DISCUSSION

HD is a devastating disorder afflicting social life and interpersonal relationships. Understanding early difficulties in deciphering gestural meanings in others and their underlying mechanisms is fundamental

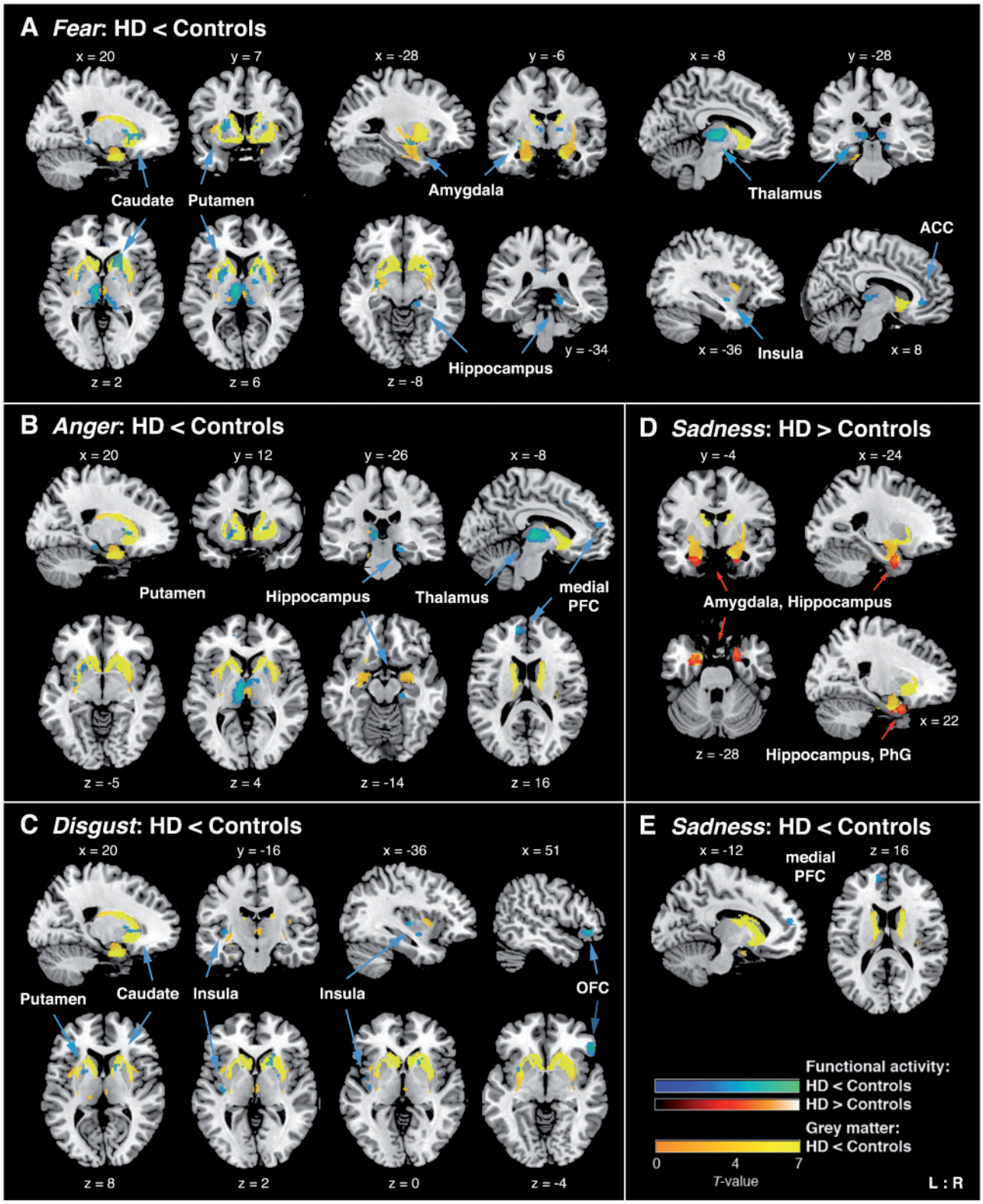


**Fig. 1** ROI showing significant BOLD signal differences between HD patients and controls in the conditions (**A**) *fear vs* neutral faces; (**B**) *anger vs* neutral; (**C**) *disgust vs* neutral; (**D**) and (**E**) *sadness vs* neutral. Lower functional activity in patients relative to controls is displayed in blue, higher activity in red (for better visualization purposes only: displayed at an uncorrected voxel threshold of $P < 0.001$). Yellow blobs indicate atrophic GM regions in HD patients compared with controls as revealed by VBM ROI analyses ($P < 0.05$, FWE corrected within ROI). ACC, anterior cingulate cortex; PFC, prefrontal cortex; OFC, orbitofrontal cortex; PhG, parahippocampal gyrus; L/R, left/right. Coordinates in MNI space; color bars represent *T*-values.

**Table 4.** ROI showing significant group differences between HD patients and controls in BOLD response to emotional *vs* neutral expressions

| Anatomical region | | MNI coordinates | | | *Z* |
|---|---|---|---|---|---|
| | | *x* | *y* | *z* | |
| Fear: HD < controls | | | | | |
| Amygdala | L | −28 | −6 | −10 | 3.72[a] |
| Hippocampus | R | 14 | −30 | −8 | 3.87 |
| Thalamus | L | −8 | −12 | 6 | 5.47 |
| | R | 14 | −2 | 4 | 4.02 |
| | R | 10 | −28 | 2 | 4.01 |
| Putamen | L | −22 | 2 | 8 | 4.63 |
| | L | −30 | −6 | −8 | 4.20 |
| | R | 18 | 12 | 2 | 4.14 |
| Caudate | R | 18 | 14 | 2 | 4.16[a] |
| Insula | L | −36 | −6 | −10 | 4.08 |
| Anterior cingulate cortex | R | 10 | 34 | −2 | 3.90 |
| Disgust: HD < controls | | | | | |
| Putamen | L | −22 | 4 | 10 | 3.83 |
| | R | 20 | 6 | 6 | 3.81 |
| Caudate | R | 16 | 10 | 6 | 3.80[a] |
| Insula | L | −36 | −14 | 2 | 4.08 |
| Orbitofrontal cortex | R | 54 | 30 | −4 | 4.77 |
| Anger: HD < controls | | | | | |
| Hippocampus | R | 18 | −24 | −14 | 4.01 |
| Thalamus | L | −8 | −20 | 6 | 5.52 |
| | R | 2 | −8 | 4 | 3.75 |
| Putamen | L | −22 | 14 | −10 | 3.78 |
| | L | −24 | 6 | 10 | 3.69 |
| | R | 22 | 6 | 4 | 3.70[a] |
| Medial prefrontal cortex | L | −10 | 54 | 16 | 4.37 |
| Sadness: HD < controls | | | | | |
| Medial prefrontal cortex | L | −12 | 54 | 16 | 4.06 |
| Sadness: HD > controls | | | | | |
| Amygdala | L | −24 | 0 | −26 | 4.46 |
| | R | 26 | 2 | −28 | 3.87[a] |
| Hippocampus | L | −22 | −2 | −32 | 3.96 |
| | R | 22 | 4 | −26 | 4.51 |
| Parahippocampal gyrus | R | 22 | 6 | −26 | 4.89 |

Results are FWE corrected at $P < 0.05$ within ROI. *Z*, maximum *Z*-value within a significant cluster. [a]Not significant after correction for atrophy (see Supplementary Table S2).

**Table 5.** Significant group differences in BOLD response outside of predicted ROI

| Anatomical region | | MNI coordinates | | | *Z* |
|---|---|---|---|---|---|
| | | *x* | *y* | *z* | |
| Fear: HD < controls | | | | | |
| Inferior frontal gyrus [BA 44] | L | −60 | 4 | 16 | 4.58 |
| PMC [BA 6], M1 [BA 4p, 4a] | L | −38 | −24 | 62 | 5.14 |
| SI [BA 3, 1, 2] | L | −40 | −30 | 54 | 5.89 |
| SMA [BA 6] | L | −4 | −14 | 48 | 4.63 |
| Middle cingulate cortex | L | −6 | −22 | 44 | 4.35 |
| Posterior cingulate cortex | L | 0 | −32 | 32 | 4.06 |
| | R | 8 | −52 | 30 | 3.73 |
| Precuneus, extends to superior parietal lobule | L | −4 | −68 | 56 | 4.65 |
| | R | 6 | −82 | 42 | 3.78 |
| Central operculum | L | −54 | 10 | 0 | 3.90 |
| Superior temporal gyrus | R | 56 | −42 | 12 | 3.61 |
| Middle temporal gyrus | R | 58 | −4 | −16 | 5.18 |
| | L | −56 | −68 | 8 | 4.78 |
| Middle temporal gyrus [V5] | R | 50 | −62 | 4 | 5.50 |
| Temporal pole | L | −52 | 6 | −2 | 3.94 |
| | R | 56 | 10 | −14 | 3.95 |
| Cuneus | L | 0 | −74 | 30 | 4.74 |
| | R | 14 | −76 | 34 | 3.60 |
| Superior occipital gyrus | L | −8 | −104 | 12 | 4.16 |
| Calcarine gyrus [BA 17] | L | −10 | −70 | 10 | 3.81 |
| Cuneus [BA 18] | L | 0 | −98 | 18 | 4.89 |
| | R | 10 | −92 | 26 | 4.67 |
| Globus pallidum | R | 18 | 6 | 4 | 4.49[a] |
| Cerebellum [Lobule V,VI,VII] | L | −22 | −70 | −26 | 4.72 |
| [Lobule V,VI] | R | 20 | −66 | −14 | 4.72 |
| Happiness: HD < controls | | | | | |
| Inferior occipital gyrus [V3v] | R | 30 | −92 | −4 | 4.03[a] |
| Middle occipital gyrus | R | 36 | −84 | 2 | 3.87[a] |
| Lingual gyrus [BA 18] | R | 22 | −92 | −10 | 3.34[a] |
| Anger: HD < controls | | | | | |
| Inferior frontal gyrus [BA 44] | L | −62 | 6 | 16 | 4.82 |
| Inferior frontal gyrus, *pars triangularis* | L | −34 | 38 | 12 | 4.00 |
| Middle frontal gyrus | L | −34 | 36 | 16 | 4.11 |
| SI [BA 3, 1, 2] | L | −44 | −30 | 52 | 5.56 |
| PMC [BA 6], extends to M1 [BA 4p, a] | L | −40 | −22 | 60 | 5.09 |
| Central operculum | L | −54 | 10 | 0 | 4.67 |
| Middle temporal gyrus, extends to right V5 | L | −58 | −64 | 8 | 4.83 |
| | R | 54 | −60 | 2 | 4.73 |
| Inferior temporal gyrus | L | −52 | −66 | −6 | 4.64 |
| Cuneus | L | 0 | −88 | 38 | 3.98[a] |
| | R | 6 | −92 | 32 | 4.00[a] |
| Cuneus [BA 18] | L | −2 | −98 | 20 | 4.25[a] |
| Inferior occiptal gyrus | L | −56 | −64 | −16 | 3.40 |
| Globus pallidum | R | 18 | 6 | 4 | 4.10 |
| Cerebellum [Lobules VI, VII] | L | −20 | −72 | −26 | 4.79 |
| [Lobules V, VI] | R | 16 | −50 | −26 | 4.26 |
| Disgust: HD < controls | | | | | |
| Inferior frontal gyrus [BA 45] | R | 52 | 32 | −2 | 4.93 |
| PMC [BA 6], M1 [BA 4p, a] | L | −40 | −24 | 62 | 3.59 |
| SI [BA 3, 1, 2] | L | −50 | −22 | 52 | 4.00 |
| Middle temporal gyrus | L | −56 | −66 | 12 | 4.61 |
| | R | 58 | −4 | −16 | 4.54 |
| Inferior temporal gyrus | L | −52 | −66 | −6 | 4.17 |
| | R | 56 | −58 | −4 | 3.65 |
| Temporal pole | R | 58 | 10 | −10 | 3.82 |
| Inferior occipital gyrus | L | −36 | −66 | −8 | 3.86 |

Results are cluster-level FWE corrected at $P < 0.05$ (uncorrected at the voxel level with $P < 0.001$) across the whole brain. *Z*, maximum *Z*-value for the anatomical area. [a]Not significant after correction for atrophy (see Supplementary Table S2). BA, Brodmann area; PMC, Premotor cortex; M1, primary motor cortex; SI, primary somatosensory cortex; SMA, supplementary motor cortex.

for our comprehension of pervasive social interaction problems in HD. In this first fMRI study on emotion processing in manifest HD, we demonstrated dysfunctions in emotion-related brain networks in the context of structural degeneration in HD, suggesting disruptions of striato-thalamo-cortical loops and potential compensation mechanisms related to disease severity.

### Emotion recognition and neural dysfunctions in emotion-related networks

In accordance with previous studies on emotion recognition abilities in HD (Henley *et al.*, 2011), our manifest patients showed deficient accuracy in recognizing negative emotions. Interestingly, patients inability to recognize *disgust* was primarily expressed as false-positive answers for anger and fear, supporting the notion that HD patients show an exaggerated form of an anger–disgust confusion that was previously reported for false-positive rates of anger recognition (Calder *et al.*, 2010). Recognition of *happiness* tended to be impaired in patients, probably due to ceiling effects in the control group, as deficient recognition of positive emotions in HD patients have been reported when more differentiated or vocal stimuli were used (Robotham *et al.*, 2011). On the neural level, group differences for the processing of *happiness* were limited to visual cortices, whereas for *fear*, *anger* and *disgust*, we revealed distributed patterns of lower functional activation in patients compared with controls. The processing of *fearful* faces revealed the most pronounced activation differences, observed in our predefined limbic ROI (i.e. ventral putamen and caudate, amygdala, hippocampus, thalamus, insula and ACC) as well as in the pallidum, cerebellum and distributed lateral prefrontal,

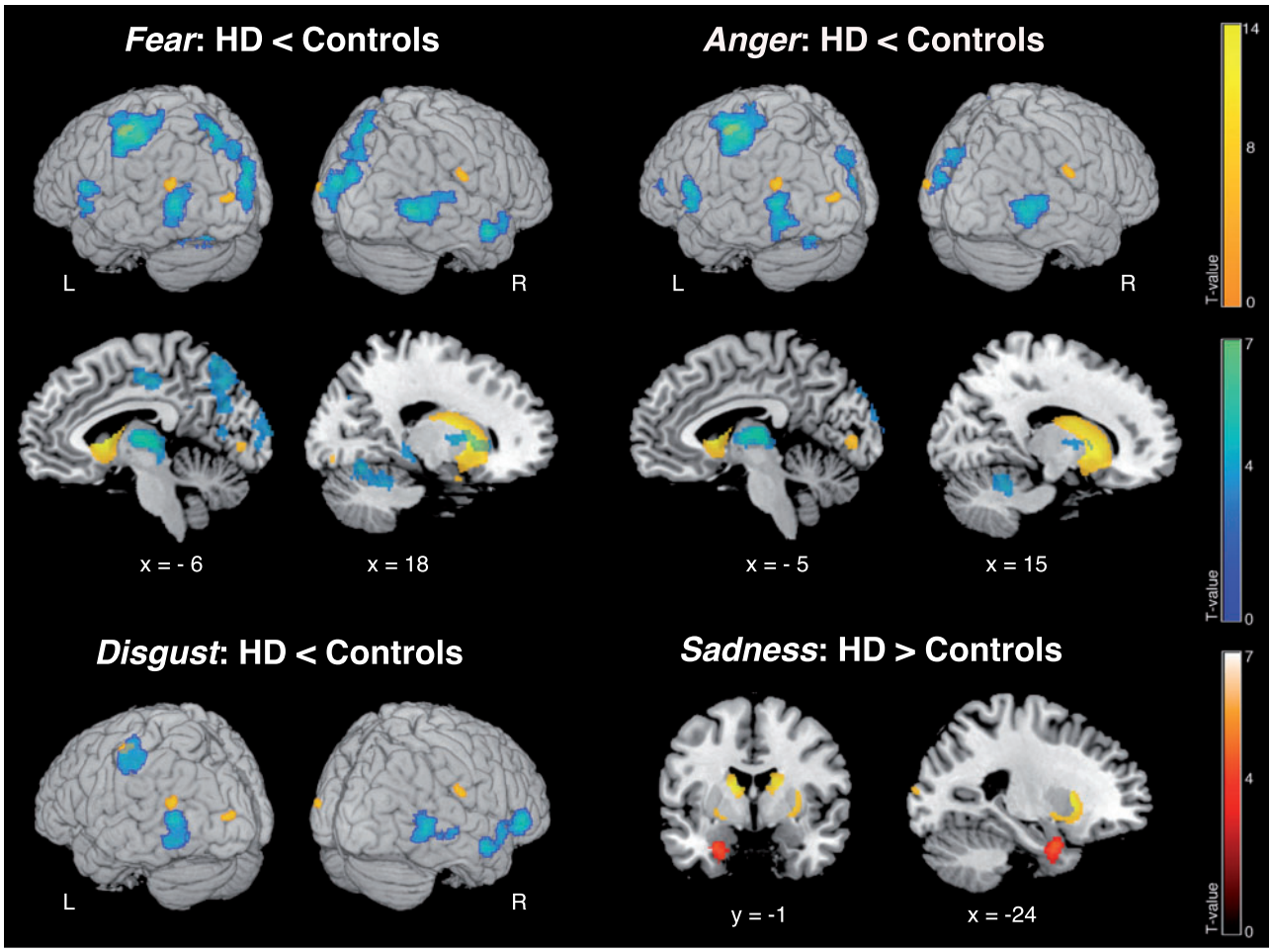


**Fig. 2** Differences in BOLD signal between HD patients and controls in the emotion recognition paradigm across the whole brain. Lower functional activity in patients relative to controls is displayed in blue, higher activity in red. Yellow blobs indicate atrophic GM regions in HD patients compared with controls as revealed by the VBM analysis across the whole brain. L/R: left/right. Coordinates in MNI space; color bars represent *T*-values.

parietal, temporal, sensorimotor and visual cortices. According to proposed basal ganglia-thalamo-cortical circuits, the ventral striatum receives input from cortices including temporal gyri, ACC, hippocampus and entorhinal cortex that are projected back to the ACC forming the 'ACC loop' (Alexander *et al.*, 1986). The ACC is connected to limbic structures such as the amygdala and insula (Craig, 2009) and is engaged in emotional tasks with cognitive demand (Phan *et al.*, 2004). Our data show emotion-related dysfunctions in these circuits in HD. Similar to the pre-manifest stage (Hennenlotter *et al.*, 2004), our patients exhibited lower BOLD response compared with controls in the left insula during the processing of *disgust* and additionally showed reduced recruitment in the right OFC and bilateral ventral putamen persisting after atrophy correction in this region. Both the insula and basal ganglia have been related to *disgust* processing (Phillips *et al.*, 1997; Sprengelmeyer *et al.*, 1998); and the reduced insular activity in patients during *fear* accords with the notion that the insula is not a specific neural substrate for disgust but rather for aversive or threat-related stimuli such as fear (Reiman *et al.*, 1997; Phan *et al.*, 2004). In comparison to recent findings on emotion processing in pre-manifest HD, Novak *et al.* (2012) detected altered neural activity in 16 pre-manifest subjects compared with controls *only* after controlling for effects of CAG repeats or proximity to disease onset, which the authors explained with the heterogeneous nature of HD arguing for baseline alterations in neural activity independent of gene dosage. Our data amplify this notion with respect to the symptomatic stage: first, we did find significant group differences without accounting for genetic dosage or factors related to disease severity, indicating that as HD progresses extensive variation in individual phenotypes converge to more general emotion-processing deficits. Second, these differences were still variable within the HD group depending partly on the extent of regional atrophy or genetic load as shown by our correlation analysis. Notably, Novak *et al.* (2012) also reported CAG-dependent functional activation in their pre-manifest sample, including negative correlations between disgust-related insular activity and CAG repeats, whereas we found positive associations in manifest HD. Similarly, significant associations between functional activity in the amygdala or hippocampus and disease-burden scores indicated an increase in BOLD response with greater disease affection (Figure 3). Considering that patients mostly showed decreased neural response, this pattern seems to be contradictory, but was reported before in functional imaging studies in HD (Feigin *et al.*, 2006; Wolf *et al.*, 2009) and might be interpreted as a compensatory, albeit less successful mechanism in more severely affected patients to counterbalance emotion-processing deficits. Generally, this direction of correlation is in line with the suggestion of an U-like temporal change of functional activity in HD with a minimum at the time of clinical conversion (Georgiou-Karistianis, 2009). In contrast, decreased activity during *fear* and *anger* in the medial thalamus connecting to prefrontal and temporal cortices (Behrens *et al.*, 2003) was associated with more pronounced thalamic volume loss, but remained robust after

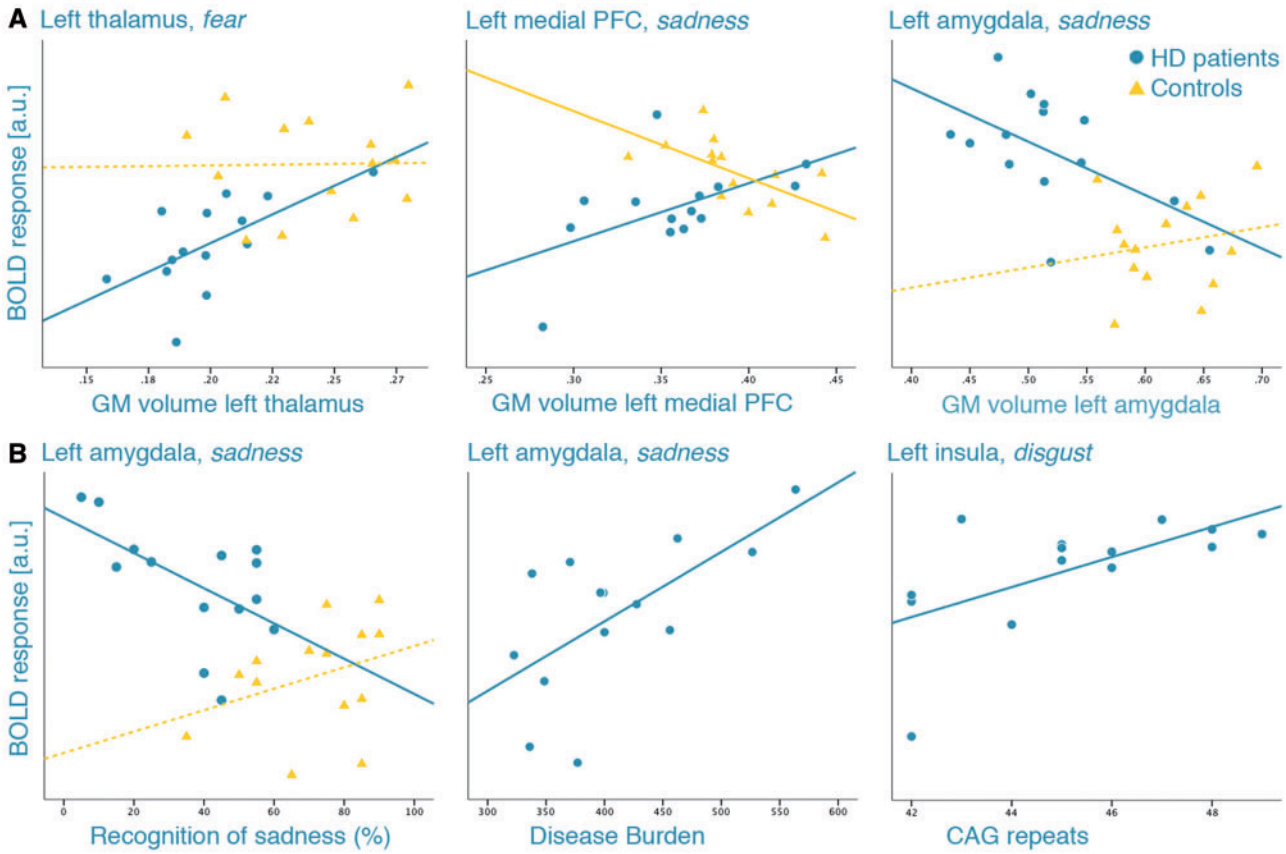


**Fig. 3** Scatter plots demonstrating the associations between functional activity in significant ROI and (**A**) regional volume loss in the same region; (**B**) behavioral task performance and genetic variables. Circles represent HD patients, triangles healthy controls; continuous lines indicate significant Pearson's $r$ at $P < 0.05$, dotted lines non-significant correlations. PFC, prefrontal cortex; a.u., arbitrary units; GM, gray matter.

correcting for thalamic atrophy. In a longitudinal PET study, Feigin *et al.* (2007) reported a decline of increased thalamic metabolism to subnormal levels when pre-manifest subjects developed symptoms, suggesting that as thalamic degeneration progresses the compensatory mechanism for early pre-manifest loss of striato-cortical activity diminishes (Feigin *et al.*, 2007). Our findings in manifest HD indicate that with increasing thalamic atrophy disruptions of its relay function between subcortical and prefrontal/temporal cortices become evident, resulting in lower functional response in distributed striatocortical networks and hence emphasize the role of the thalamus in emotion processing as previously shown for other cognitive domains in HD (Kassubek *et al.*, 2005). We also found reduced neural activity in HD patients compared with controls in occipito-temporal and parietal regions, including somatosensory and central opercular cortices. Although we controlled for simple sensory processing by contrasting emotional stimuli to neutral expressions, activation in visual association areas tends to be elicited more extensively by complex stimuli with emotional relevance than face processing alone (Phan *et al.*, 2002). The lower neural activation in patients in visual areas indicate deficient early perceptual processing of emotional-relevant stimuli in HD that is necessary to construct representations of facial features before inferring the meaning about an emotion (Adolphs, 2002). Somatosensory cortices seem to play a critical role in emotion recognition as the representation of the emotional response in primary and secondary somatosensory cortices can facilitate the ability to assemble information on the emotion seen in others (Adolphs *et al.*, 2000). Hence, reduced neural activity in parietal regions might contribute to emotion recognition deficits in HD.

### Increased limbic activity and processing of sadness

We further observed increased BOLD response in patients during videos displaying *sadness* that was substantial after correcting for atrophy in the left amygdala, bilateral hippocampus and right parahippocampal gyrus. Enhanced neural activation is usually interpreted as compensatory recruitment representing primary dysfunctions with respect to cortical degeneration or secondary compensatory processes due to striatal deficits in HD (Georgiou-Karistianis, 2009; Paulsen, 2009). Our correlation analysis suggests an increase of amygdala activity with more advanced amygdala atrophy and higher disease burden. Because of the fact that amygdala activity was the only functional data associated with task performance, it is plausible to think of a compensatory though counterproductive attempt in patients at recruiting more extensively this region. Increased amygdala response particularly during the processing of sad expressions has been reported in patients with major depressive disorder (Surguladze *et al.*, 2005; Victor *et al.*, 2010) and was associated with deficits in explicit labeling of negative emotions (van Wingen *et al.*, 2011), which might be related to the findings in our HD patients showing depressive mood symptoms. However, in depressed patients, a more distributed pattern of enhanced neural activity in networks important for the processing of emotional stimuli (e.g. putamen and occipito-temporal regions) seems to be involved (Surguladze *et al.*, 2005). Increased amygdala response to facial stimuli has also been shown in other neurodegenerative diseases such as Alzheimer's disease (AD) and was associated with irritability and aggression in AD (Wright *et al.*, 2007) indicating a clinical significance of this finding for features that are also common in HD. A functional connectivity analysis using resting-state fMRI in healthy subjects revealed distinct connectivity patterns within the amygdala,

in which laterobasal subdivisions predicted activity in temporal and frontal regions, while the centromedial part predicted primarily striatal activity (Roy *et al.*, 2009). Similarly, in our analysis, reduced centromedial amygdala response during *fear* was accompanied by lower striatal activity, while we found lower recruitment in the mPFC in addition to the enhanced activity in the laterobasal amygdala during *sadness*. The mPFC is involved in cognitive aspects of emotion processing (e.g. attention or identification of emotion) and might serve as a 'top-down' modulator of intense emotional responses, generated for instance by the amygdala (Phan *et al.*, 2004). Since lower functional response in the mPFC was associated with lower GM density in patients, the enhancement in BOLD response in subcortical limbic structures may arise from a lack of higher order prefrontal inhibition of intense subcortical activity. However, decreased activity in the mPFC was also observed for *anger* (and in other prefrontal areas for negative emotions) in the absence of subcortical hyperactivation. Thus, it remains unclear why these specific effects were observed only for *sadness* but not any other negative emotion, as we did not detect any disproportionate impairment on the behavioral level. Error type analysis showed that patients misclassified sad videos more frequently as fear and anger, which might partly explain the increase in amygdala activity, though compared with controls false positives were only significant for neutral expressions. Another possible explanation might be that the videos expressing sadness used in our study might have been experienced as more emotive by our patients. As deficient recognition accuracy for *sadness* is less consistently reported than for other negative emotions in manifest HD (Montagne *et al.*, 2006; Calder *et al.*, 2010; Henley *et al.*, 2011), it is also conceivable that the neural basis for this particular emotion may follow different functional maintenance strategies. The exact neural mechanism underlying this striking finding for *sadness* remains elusive, and since both fMRI studies in pre-manifest HD did not employ sad expressions to compare with our data, future imaging studies will need to elucidate the stability of our findings.

## LIMITATIONS AND CONCLUSIONS

A potential limitation of this study is that our HD sample showed impairments in other cognitive domains than emotion recognition alone. Progressive cognitive decline, especially in the manifest stage, is intrinsic to HD (Paulsen, 2011), making the investigation of definite functional networks difficult. However, we did not detect systematic variations neither of recognition accuracy nor functional data in respective ROI with cognitive measures in patients. Moreover, our aim was to investigate the neural mechanism underlying emotion-processing deficits in HD, for which we used an explicit emotion recognition paradigm with dynamic stimuli (rather than less provoking static images) to induce conscious emotion processing and did not omit incorrect trials but assessed systematic co-variations with behavioral performance. After including only patients with correct total task performance above 50% results remained largely unchanged, and the additionally observed activity in the ACC and middle frontal gyrus is compatible with findings reported in pre-manifest HD for disgust and anger processing (Novak *et al.* 2012). However, it would have been interesting to assess more systematically the difference in neural response between correct and incorrect trials in order to reveal more differential aspects of emotion processing in HD. Since patients showed severe impairments in behavioral performance, as expected in the manifest stage of HD, these analyses are not feasible with the current data and need to be addressed in future studies using more differentiated stimuli (e.g. varying intensity or task difficulty). Further, because of widespread structural degeneration particularly in the manifest HD stage, functional data will inherently be confounded by anatomical tissue loss. We aimed to overcome this issue by combining both functional and structural data, revealing differential aspects between regional tissue loss and functional alterations. Although we used a rather conservative correction method in terms of ROI-based VBM analysis, this approach might also reduce the sensitivity in detecting activation differences in relevant areas in contrast to voxel-wise covariate methods (Oakes *et al.*, 2007).

In conclusion, we have shown that impaired emotion processing is associated with lower functional activity in widespread subcortical and cortical regions in manifest HD. Degeneration, particularly in subcortical structures, seems to mediate functional decline, but cannot fully explain the observed alterations suggesting extensive disruptions of basal ganglia-thalamo-cortical circuits. Increase in functional recruitment as observed in the amygdala involves greater disease affection along with a lack of higher order inhibition. With respect to HD's heterogeneity, deficient emotion processing is highly variable even in the manifest stage but seems to converge to a more general impairment, both behaviorally and functionally. For future studies, it will be desirable to use more differentiated stimuli of emotional valences in conjunction with detailed ratings of respective emotions (e.g. intensity and emotiveness) to validate our findings and to elucidate more differential aspects of the neural basis of emotion processing in HD.

## SUPPLEMENTARY DATA

Supplementary data are available at *SCAN* online.

## REFERENCES


Adolphs, R. (2002). Neural systems for recognizing emotion. *Current Opinion in Neurobiology*, *12*, 169–77.

Adolphs, R., Damasio, H., Tranel, D., Cooper, G., Damasio, A.R. (2000). A role for somatosensory cortices in the visual recognition of emotion as revealed by three-dimensional lesion mapping. *Journal of Neuroscience*, *20*, 2683–90.

Alexander, G.E., DeLong, M.R., Strick, P.L. (1986). Parallel organization of functionally segregated circuits linking basal ganglia and cortex. *Annual Review of Neuroscience*, *9*, 357–81.

Amunts, K., Kedo, O., Kindler, M., et al. (2005). Cytoarchitectonic mapping of the human amygdala, hippocampal region and entorhinal cortex: intersubject variability and probability maps. *Anatomy and Embryology (Berl)*, *210*, 343–52.

Anders, S., Sack, B., Pohl, A., et al. (2012). Compensatory premotor activity during affective face processing in subclinical carriers of a single mutant Parkin allele. *Brain*, *135*, 1128–40.

Ashburner, J., Friston, K.J. (2000). Voxel-based morphometry—the methods. *Neuroimage*, *11*, 805–21.

Aylward, E.H., Sparks, B.F., Field, K.M., et al. (2004). Onset and rate of striatal atrophy in preclinical Huntington disease. *Neurology*, *63*, 66–72.

Behrens, T.E., Johansen-Berg, H., Woolrich, M.W., et al. (2003). Non-invasive mapping of connections between human thalamus and cortex using diffusion imaging. *Nature Neuroscience*, *6*, 750–7.

Benecke, C., Vogt, T., Bock, A., Koschier, A., Peham, D. (2008). Emotionserleben und Emotionsregulation und ihr Zusammenhang mit psychischer Symptomatik. PPmP—Psychotherapie Psychosomatik Medizinische Psychologie.

Calder, A.J., Keane, J., Young, A.W., Lawrence, A.D., Mason, S., Barker, R.A. (2010). The relation between anger and different forms of disgust: implications for emotion recognition impairments in Huntington's disease. *Neuropsychologia*, *48*, 2719–29.

Craig, A.D. (2009). How do you feel—now? The anterior insula and human awareness. *Nature Reviews. Neuroscience*, *10*, 59–70.

Eickhoff, S.B., Heim, S., Zilles, K., Amunts, K. (2006). Testing anatomically specified hypotheses in functional imaging using cytoarchitectonic maps. *Neuroimage*, *32*, 570–82.

Eickhoff, S.B., Stephan, K.E., Mohlberg, H., et al. (2005). A new SPM toolbox for combining probabilistic cytoarchitectonic maps and functional imaging data. *Neuroimage*, *25*, 1325–35.

Feigin, A., Ghilardi, M.F., Huang, C., et al. (2006). Preclinical Huntington's disease: compensatory brain responses during learning. *Annals of Neurology*, *59*, 53–9.

Feigin, A., Tang, C., Ma, Y., et al. (2007). Thalamic metabolism and symptom onset in preclinical Huntington's disease. *Brain*, *130*, 2858–67.

Folstein, M.F., Folstein, S.E., McHugh, P.R. (1975). "Mini-mental state". A practical method for grading the cognitive state of patients for the clinician. *Journal of Psychiatric Research*, *12*, 189–98.

Friston, K.J., Frith, C.D., Turner, R., Frackowiak, R.S. (1995). Characterizing evoked hemodynamics with fMRI. *Neuroimage*, *2*, 157–65.

Fusar-Poli, P., Placentino, A., Carletti, F., et al. (2009). Functional atlas of emotional faces processing: a voxel-based meta-analysis of 105 functional magnetic resonance imaging studies. *Journal of Psychiatry & Neuroscience*, *34*, 418–32.

Georgiou-Karistianis, N. (2009). A peek inside the Huntington's brain: will functional imaging take us one step closer in solving the puzzle? *Experimental Neurology*, *220*, 5–8.

Good, C.D., Johnsrude, I.S., Ashburner, J., Henson, R.N., Friston, K.J., Frackowiak, R.S. (2001). A voxel-based morphometric study of ageing in 465 normal adult human brains. *Neuroimage*, *14*, 21–36.

Gray, J.M., Young, A.W., Barker, W.A., Curtis, A., Gibson, D. (1997). Impaired recognition of disgust in Huntington's disease gene carriers. *Brain*, *120*(Pt 11), 2029–38.

Haidt, J., McCauley, C., Rozin, P. (1994). Individual differences in sensitivity to disgust: a scale sampling seven domains of disgust elicitors. *Personality and Individual Differences*, *16*, 701–13.

Henley, S.M., Novak, M.J., Frost, C., King, J., Tabrizi, S.J., Warren, J.D. (2011). Emotion recognition in Huntington's disease: a systematic review. *Neuroscience and Biobehavioral Reviews*, *36*, 237–53.

Henley, S.M., Wild, E.J., Hobbs, N.Z., et al. (2008). Defective emotion recognition in early HD is neuropsychologically and anatomically generic. *Neuropsychologia*, *46*, 2152–60.

Hennenlotter, A., Schroeder, U., Erhard, P., et al. (2004). Neural correlates associated with impaired disgust processing in pre-symptomatic Huntington's disease. *Brain*, *127*, 1446–53.

Huntington Study Group (1996). Unified Huntington's Disease Rating Scale: reliability and consistency. *Movement Disorders*, *11*, 136–42.

Ille, R., Schafer, A., Scharmuller, W., et al. (2011). Emotion recognition and experience in Huntington disease: a voxel-based morphometry study. *Journal of Psychiatry & Neuroscience*, *36*, 100143.

Johnson, S.A., Stout, J.C., Solomon, A.C., et al. (2007). Beyond disgust: impaired recognition of negative emotions prior to diagnosis in Huntington's disease. *Brain*, *130*, 1732–44.

Kassubek, J., Juengling, F.D., Ecker, D., Landwehrmeyer, G.B. (2005). Thalamic atrophy in Huntington's disease co-varies with cognitive performance: a morphometric MRI analysis. *Cerebral Cortex*, *15*, 846–53.

Kipps, C.M., Duggins, A.J., McCusker, E.A., Calder, A.J. (2007). Disgust and happiness recognition correlate with anteroventral insula and amygdala volume respectively in preclinical Huntington's disease. *Journal of Cognitive Neuroscience*, *19*, 1206–17.

Kircher, T., Pohl, A., Krach, S., et al. (2012). Affect-specific activation of shared networks for perception and execution of facial expressions. *Social Cognitive and Affective Neuroscience*, [21 February 2012, Epub ahead of print].

Maldjian, J.A., Laurienti, P.J., Kraft, R.A., Burdette, J.H. (2003). An automated method for neuroanatomic and cytoarchitectonic atlas-based interrogation of fMRI data sets. *Neuroimage*, *19*, 1233–9.

Montagne, B., Kessels, R.P., Kammers, M.P., et al. (2006). Perception of emotional facial expressions at different intensities in early-symptomatic Huntington's disease. *European Neurology*, *55*, 151–4.

Nelson, H.E. (1976). A modified card sorting test sensitive to frontal lobe defects. *Cortex*, *12*, 313–24.

Novak, M.J., Warren, J.D., Henley, S.M., Draganski, B., Frackowiak, R.S., Tabrizi, S.J. (2012). Altered brain mechanisms of emotion processing in pre-manifest Huntington's disease. *Brain*, *135*, 1165–79.

Oakes, T.R., Fox, A.S., Johnstone, T., Chung, M.K., Kalin, N., Davidson, R.J. (2007). Integrating VBM into the general linear model with voxelwise anatomical covariates. *Neuroimage*, *34*, 500–8.

Paulsen, J.S. (2009). Functional imaging in Huntington's disease. *Experimental Neurology*, *216*, 272–7.

Paulsen, J.S. (2011). Cognitive impairment in Huntington disease: diagnosis and treatment. *Current Neurology and Neuroscience Reports*, *11*, 474–83.

Paulsen, J.S., Nopoulos, P.C., Aylward, E., et al. (2010). Striatal and white matter predictors of estimated diagnosis for Huntington disease. *Brain Research Bulletin*, *82*, 201–7.

Penney, J.B.Jr, Vonsattel, J.P., MacDonald, M.E., Gusella, J.F., Myers, R.H. (1997). CAG repeat number governs the development rate of pathology in Huntington's disease. *Annals of Neurology*, *41*, 689–92.

Phan, K.L., Wager, T., Taylor, S.F., Liberzon, I. (2002). Functional neuroanatomy of emotion: a meta-analysis of emotion activation studies in PET and fMRI. *Neuroimage*, *16*, 331–48.

Phan, K.L., Wager, T.D., Taylor, S.F., Liberzon, I. (2004). Functional neuroimaging studies of human emotions. *CNS Spectrums*, *9*, 258–66.

Phillips, M.L., Young, A.W., Senior, C., et al. (1997). A specific neural substrate for perceiving facial expressions of disgust. *Nature*, *389*, 495–8.

Reiman, E.M., Lane, R.D., Ahern, G.L., et al. (1997). Neuroanatomical correlates of externally and internally generated human emotion. *American Journal of Psychiatry*, *154*, 918–25.

Robotham, L., Sauter, D.A., Bachoud-Levi, A.C., Trinkler, I. (2011). The impairment of emotion recognition in Huntington's disease extends to positive emotions. *Cortex*, *47*, 880–4.

Roy, A.K., Shehzad, Z., Margulies, D.S., et al. (2009). Functional connectivity of the human amygdala using resting state fMRI. *Neuroimage*, *45*, 614–26.

Scahill, R.I., Hobbs, N.Z., Say, M.J., et al. (2011). Clinical impairment in premanifest and early Huntington's disease is associated with regionally specific atrophy. *Human Brain Mapping*, *34*, 519–29.

Shoulson, I., Fahn, S. (1979). Huntington disease: clinical care and evaluation. *Neurology*, *29*, 1–3.

Snaith, R.P., Constantopoulos, A.A., Jardine, M.Y., McGuffin, P. (1978). A clinical scale for the self-assessment of irritability. *British Journal of Psychiatry*, *132*, 164–71.

Sprengelmeyer, R., Rausch, M., Eysel, U.T., Przuntek, H. (1998). Neural structures associated with recognition of facial expressions of basic emotions. *Proceedings of Biological Sciences*, *265*, 1927–31.

Sprengelmeyer, R., Schroeder, U., Young, A.W., Epplen, J.T. (2006). Disgust in pre-clinical Huntington's disease: a longitudinal study. *Neuropsychologia*, *44*, 518–33.

Surguladze, S., Brammer, M.J., Keedwell, P., et al. (2005). A differential pattern of neural response toward sad versus happy facial expressions in major depressive disorder. *Biological Psychiatry*, *57*, 201–9.

Tabrizi, S.J., Langbehn, D.R., Leavitt, B.R., et al. (2009). Biological and clinical manifestations of Huntington's disease in the longitudinal TRACK-HD study: cross-sectional analysis of baseline data. *Lancet Neurology*, *8*, 791–801.

Truong, M.K. (1993). *Short Wisconsin Card Sorting Test nach Nelson 1976*, Version 1.1. Wuppertal: Universität-GHS Wuppertal, Klinische Psychologie.

Tzourio-Mazoyer, N., Landeau, B., Papathanassiou, D., et al. (2002). Automated anatomical labeling of activations in SPM using a macroscopic anatomical parcellation of the MNI MRI single-subject brain. *Neuroimage*, *15*, 273–89.

van Wingen, G.A., van Eijndhoven, P., Tendolkar, I., Buitelaar, J., Verkes, R.J., Fernandez, G. (2011). Neural basis of emotion recognition deficits in first-episode major depression. *Psychological Medicine*, *41*, 1397–405.

Victor, T.A., Furey, M.L., Fromm, S.J., Ohman, A., Drevets, W.C. (2010). Relationship between amygdala responses to masked faces and mood state and treatment in major depressive disorder. *Archives of General Psychiatry*, *67*, 1128–38.

Vonsattel, J.P. (2008). Huntington disease models and human neuropathology: similarities and differences. *Acta Neuropathology*, *115*, 55–69.

Watson, D., Clark, L.A., Tellegen, A. (1988). Development and validation of brief measures of positive and negative affect: the PANAS scales. *Journal of Personality and Social Psychology*, *54*, 1063–70.

Wolf, R.C., Vasic, N., Schonfeldt-Lecuona, C., Ecker, D., Landwehrmeyer, G.B. (2009). Cortical dysfunction in patients with Huntington's disease during working memory performance. *Human Brain Mapping*, *30*, 327–39.

Wright, C.I., Dickerson, B.C., Feczko, E., Negeira, A., Williams, D. (2007). A functional magnetic resonance imaging study of amygdala responses to human faces in aging and mild Alzheimer's disease. *Biological Psychiatry*, *62*, 1388–95.